Research Square

Preprints are preliminary reports that have not undergone peer review.
They should not be considered conclusive, used to inform clinical practice,
or referenced by the media as validated information.

In Silico Identification of Spironolactone as a Walker B Associated Candidate in the NLRP3 NACHT ATPase Domain

Mishel Abdullah

mishelabdullahh@gmail.com

All India Institute of Medical Sciences, New Delhi https://orcid.org/0009-0007-6326-8572

Jayadevan K

All India Institute of Medical Sciences, New Delhi https://orcid.org/0009-0003-9137-471X

Amalkrishnan Therayil

All India Institute of Medical Sciences, New Delhi https://orcid.org/0009-0006-0781-376X

Alhan Faiza

PSG College of Atrs and Science, Coimbatore https://orcid.org/0009-0003-6730-1588

Research Article

Keywords: NLRP3 inflammasome, NACHT domain, ATPase inhibition, Walker B motif, Spironolactone, MCC950 (CRID3)

Posted Date: April 7th, 2026

DOI: https://doi.org/10.21203/rs.3.rs-9318173/v1

License: This work is licensed under a Creative Commons Attribution 4.0 International License.
Read Full License

Additional Declarations: The authors declare no competing interests.

Abstract

The NLRP3 inflammasome is a cytosolic complex whose activation depends on ATP binding and hydrolysis within the central NACHT domain. MCC950 (CRID3) targets this ATPase region and engages residues proximal to the Walker B motif, providing a structural benchmark for inhibitor discovery. Here, we performed molecular docking based virtual screening of 100 FDA-approved small molecules against the NLRP3 NACHT ATP-binding cavity using the cryo-EM structure of NLRP3 bound to CRID3 (PDB ID: 7PZC). Redocking of MCC950 yielded a best binding energy of −9.79 kcal/mol and reproduced localization within the Walker B–associated sub-pocket, including a predicted hydrogen bond with Asp274 and a buried surface area of 455.68 Å². Top-ranked compounds exhibited predicted binding energies between −10.7 and −9.6 kcal/mol; however, spatial analysis showed that several localized outside the MCC950-associated site. Incorporation of centroid deviation, buried surface area, and proximity to Asp274 enabled prioritization of structurally aligned candidates. Spironolactone demonstrated the closest alignment to MCC950, with a docking score of −9.99 kcal/mol, centroid deviation of 1.35 Å, comparable burial (460.35 Å²), and predicted interaction with Asp274. These results identify Spironolactone as a structurally aligned NACHT-binding candidate warranting experimental validation.

Introduction

The NLRP3 inflammasome is a cytosolic multiprotein complex that mediates caspase-1 activation and the maturation of interleukin-1β (IL-1β) and interleukin-18 (IL-18). Aberrant NLRP3 activation contributes to inflammatory and metabolic disorders including cryopyrin-associated periodic syndromes (CAPS), gout, type 2 diabetes, and neuroinflammatory diseases (1). The central NACHT domain of NLRP3 functions as an ATPase that drives inflammasome assembly and contains conserved Walker A and Walker B motifs required for nucleotide binding and hydrolysis (2), making the ATP-binding pocket a mechanistically relevant therapeutic target.

MCC950 (CRID3) is a potent and selective NLRP3 inhibitor that directly targets the NACHT domain and suppresses ATP hydrolysis, with evidence supporting engagement near the Walker B motif (3, 4). Structural studies have provided a framework for understanding inhibitor interactions within this ATPase region (2). However, MCC950 has not advanced clinically, underscoring the need to identify alternative compounds capable of targeting the same functional sub-pocket.

Here, we applied structure-based virtual screening of FDA-approved small molecules against the NLRP3 NACHT ATP-binding cavity using MCC950 as a structural benchmark. Compounds were prioritized based on predicted binding energy and structural alignment with the Walker B–associated sub-pocket. This strategy provides a hypothesis-generating approach for identifying repurposable candidates targeting the NLRP3 ATPase domain.

Methods

Protein Structure Preparation

The cryo-electron microscopy structure of the human NLRP3 decamer in complex with the inhibitor CRID3 (MCC950) (PDB ID: 7PZC) was obtained from the Protein Data Bank (5). A single NACHT-containing protomer was extracted from the decameric assembly for docking analysis to avoid inter-chain steric interference. The co-resolved CRID3 molecule, water molecules, and non-protein heteroatoms were removed prior to preparation. Polar hydrogens were added, and Gasteiger partial charges were assigned using AutoDockTools (6). The prepared receptor structure was exported in PDBQT format.

Binding Site Definition

The docking grid was centered on the CRID3-binding cavity within the NACHT ATPase domain as observed in the 7PZC structure (5). Grid dimensions were defined to encompass the ATP-binding pocket, including the Walker A and Walker B motifs. The same grid coordinates were used for redocking and virtual screening to ensure methodological consistency.

Ligand Library Preparation

A library of 100 FDA-approved small molecules (molecular weight ≤ 700 Da) was curated from DrugBank. Three-dimensional structures were generated using Open Babel (7). Hydrogen atoms were added and Gasteiger charges assigned. Each ligand was converted to PDBQT format using AutoDockTools. A single dominant protonation state at physiological pH was retained for docking.

Molecular Docking

Docking simulations were performed using AutoDock Vina (8). Virtual screening was conducted with an exhaustiveness value of 12 and default output modes. MCC950 was redocked under identical conditions, with exhaustiveness increased to 32 to confirm convergence of binding poses. For each ligand, the lowest-energy conformation was selected for downstream analysis.

Post-Docking Structural Analysis

Docking results were ranked according to predicted binding energy (kcal/mol). Spatial similarity relative to redocked MCC950 was evaluated by calculating centroid distances using UCSF ChimeraX (9). Solvent-accessible buried surface area between ligand and protein was calculated using the ChimeraX measure buriedarea function with a probe radius of 1.4 Å. Protein–ligand interaction profiles, including hydrophobic interactions, hydrogen bonds, and salt bridges, were determined using the Protein–Ligand

Interaction Profiler (PLIP) v2.4.0 (10). All reported binding energies and interactions represent computational predictions derived from rigid receptor docking.

Results

Redocking of the Benchmark Inhibitor MCC950

To validate the docking workflow, the well-characterized NLRP3 inhibitor MCC950 was redocked into the NACHT ATP-binding cavity using an expanded grid and increased exhaustiveness to ensure convergence. Redocking yielded a best binding energy of − 9.79 kcal/mol, and multiple low-energy conformations clustered within a narrow energy window of less than 1 kcal/mol, indicating reproducibility of the docking protocol. The predicted pose localized within the ATP-binding cavity in close proximity to the Walker B motif.

Interaction analysis revealed a hydrogen bond with Asp274, a key residue within the Walker B region implicated in ATP hydrolysis. The buried solvent-accessible surface area between MCC950 and the NACHT domain was calculated to be 455.68 Å², indicating substantial burial within the nucleotide-binding cavity. In addition, hydrophobic interactions were observed with ILE234, LEU413, TRP416, and PHE508, forming a stabilizing hydrophobic environment surrounding the ligand. Together, these observations recapitulate the expected localization of MCC950 within the ATPase cavity and establish a structural benchmark for subsequent comparative screening.

Virtual Screening of FDA-Approved Drugs

A curated library of 100 FDA-approved small molecules with molecular weights of 700 Da or less was screened against the NACHT ATP-binding pocket using identical docking parameters. The top ten ranked compounds exhibited predicted binding energies ranging from − 10.7 to − 9.6 kcal/mol (Fig. 1). Although several compounds demonstrated more favorable docking scores than MCC950, spatial inspection revealed that multiple high-scoring ligands occupied alternative sub-pockets within the NACHT cavity rather than the MCC950-associated region.

To distinguish energetically favorable yet spatially irrelevant poses from structurally aligned candidates, additional metrics were incorporated into the analysis. These included centroid deviation relative to redocked MCC950, buried solvent-accessible surface area, and proximity to the Walker B residue Asp274. This multi-parameter filtering approach enabled prioritization of compounds that demonstrated not only favorable predicted binding energy but also structural congruence with the benchmark inhibitor.

Identification of Spironolactone as a Walker B–Associated Candidate

Among the screened compounds, Spironolactone demonstrated the strongest structural similarity to MCC950. Spironolactone exhibited a docking score of − 9.99 kcal/mol, a centroid deviation of 1.35 Å relative to MCC950, and a buried surface area of 460.35 Å². The minimal centroid deviation indicates near-identical spatial positioning within the ATP-binding cavity, while the comparable buried surface area supports similar depth of pocket occupancy.

Interaction profiling identified a hydrogen bond between Spironolactone and Asp274, mirroring the Walker B interaction observed for MCC950 (Fig. 2). Conserved hydrophobic contacts with ILE234, LEU413, TRP416, and PHE508 further confirmed localization within the MCC950-associated sub-pocket. In addition, a predicted salt bridge with ARG167 was observed, suggesting supplementary electrostatic stabilization within the cavity. Collectively, these findings indicate that Spironolactone occupies the same NACHT ATP-binding sub-pocket and engages the Walker B region in a structurally analogous manner to MCC950.

Secondary Candidates and Spatial Discrimination

Montelukast, Donepezil, and Ketoconazole demonstrated moderate spatial overlap with MCC950, with centroid deviations between 3.9 and 4.3 Å, and localized within the ATP-binding cavity, although their alignment relative to the Walker B region was less precise. In contrast, several high-scoring ligands, including Apixaban, Imatinib, and Etoposide, displayed centroid deviations exceeding 17 Å, indicating binding to distinct regions of the NACHT cavity and limited proximity to Walker B residues. These findings emphasize that docking score alone does not reliably predict mechanistic relevance to the nucleotide-binding region.

Structural Summary

Taken together, the data identify Spironolactone as the compound demonstrating the closest structural alignment with the MCC950-associated NACHT ATP-binding sub-pocket. This alignment is supported by comparable docking energy, minimal centroid deviation, similar buried surface area, and predicted engagement of the Walker B residue Asp274. All reported interactions and binding energies represent computational predictions derived from rigid receptor docking and should be considered hypothesis-generating pending biochemical and functional validation.

Discussion

Redocking of MCC950 into the NACHT ATP-binding cavity reproduced a binding mode proximal to the Walker B region, including predicted interaction with Asp274 and substantial burial within the nucleotide-binding pocket. This observation is consistent with prior biochemical and structural studies demonstrating that MCC950 targets the NACHT domain and interferes with ATP hydrolysis (4, 5). The clustering of low-energy poses within a narrow energy window further supports internal consistency of the docking workflow. While rigid receptor docking cannot fully capture conformational dynamics, the recovery of a Walker B–associated pose provides a structural benchmark for comparative screening.

Virtual screening of 100 FDA-approved compounds yielded several ligands with docking scores numerically more favorable than MCC950. However, centroid distance and spatial mapping revealed that many top-scoring compounds localized to alternative sub-pockets within the NACHT cavity rather than the MCC950-associated site. This reinforces a well-recognized limitation of docking-based ranking: predicted binding energy alone does not establish mechanistic relevance to a functional motif. Incorporating spatial overlap, buried surface area, and proximity to Walker B residues enabled prioritization of candidates with structural alignment to the benchmark inhibitor rather than reliance on score magnitude alone.

Among screened compounds, Spironolactone demonstrated the strongest structural convergence with MCC950. The minimal centroid deviation (1.35 Å), comparable buried surface area, and predicted hydrogen bond interaction with Asp274 collectively indicate occupation of the same NACHT sub-pocket. Conserved hydrophobic interactions with ILE234, LEU413, TRP416, and PHE508 further support engagement of the established inhibitor-binding environment. Notably, Spironolactone additionally formed a predicted salt bridge with ARG167, suggesting supplementary electrostatic stabilization that was not observed in the MCC950 docking pose. Although docking does not establish inhibition or functional suppression, these structural similarities suggest that Spironolactone may interact with the ATPase region in a manner analogous to MCC950.

Several limitations should be acknowledged. The docking simulations were performed using a rigid receptor model derived from a cryo-EM structure of the NLRP3 decamer, and only a single protomer was used for computational tractability. Conformational flexibility, oligomeric interface effects, solvent dynamics, and ATP competition were not modeled. Furthermore, docking scores from AutoDock Vina have an expected uncertainty of approximately ± 1 kcal/mol, limiting fine discrimination between closely ranked compounds (8). Therefore, the present findings should be interpreted as structural predictions rather than evidence of functional modulation.

In summary, this in silico triage approach identified Spironolactone as a structurally aligned candidate within the MCC950-associated NACHT ATP-binding sub-pocket. The predicted engagement of the Walker B region supports a mechanistically relevant hypothesis that warrants further biochemical and cellular validation. These findings demonstrate that spatial alignment with a mechanistically defined sub-pocket provides a more biologically relevant prioritization strategy than docking score alone.

References

1. Swanson KV, Deng M, Ting JPY. The NLRP3 inflammasome: molecular activation and regulation to therapeutics. Nat Rev Immunol. 2019 Aug;19(8):477–89. doi:10.1038/s41577-019-0165-0
2. Sharif H, Wang L, Wang WL, Magupalli VG, Andreeva L, Qiao Q, et al. Structural mechanism for NEK7-licensed activation of NLRP3 inflammasome. Nature. 2019 Jun 20;570(7761):338–43. doi:10.1038/s41586-019-1295-z

3. Coll RC, Robertson AAB, Chae JJ, Higgins SC, Muñoz-Planillo R, Inserra MC, et al. A small-molecule inhibitor of the NLRP3 inflammasome for the treatment of inflammatory diseases. Nat Med. 2015 Mar;21(3):248–55. doi:10.1038/nm.3806
4. Tapia-Abellán A, Angosto-Bazarra D, Martínez-Banaclocha H, De Torre-Minguela C, Cerón-Carrasco JP, Pérez-Sánchez H, et al. MCC950 closes the active conformation of NLRP3 to an inactive state. Nat Chem Biol. 2019 Jun;15(6):560–4. doi:10.1038/s41589-019-0278-6
5. Dekker C, Mattes H, Wright M, Boettcher A, Hinniger A, Hughes N, et al. Crystal Structure of NLRP3 NACHT Domain With an Inhibitor Defines Mechanism of Inflammasome Inhibition. J Mol Biol. 2021 Dec;433(24):167309. doi:10.1016/j.jmb.2021.167309
6. Morris GM, Huey R, Lindstrom W, Sanner MF, Belew RK, Goodsell DS, et al. AutoDock4 and AutoDockTools4: Automated docking with selective receptor flexibility. J Comput Chem. 2009 Dec;30(16):2785–91. doi:10.1002/jcc.21256
7. O'Boyle NM, Banck M, James CA, Morley C, Vandermeersch T, Hutchison GR. Open Babel: An open chemical toolbox. J Cheminformatics. 2011 Dec;3(1):33. doi:10.1186/1758-2946-3-33
8. Trott O, Olson AJ. AutoDock Vina: Improving the speed and accuracy of docking with a new scoring function, efficient optimization, and multithreading. J Comput Chem. 2010 Jan 30;31(2):455–61. doi:10.1002/jcc.21334
9. Pettersen EF, Goddard TD, Huang CC, Meng EC, Couch GS, Croll TI, et al. UCSF ChimeraX : Structure visualization for researchers, educators, and developers. Protein Sci. 2021 Jan;30(1):70–82. doi:10.1002/pro.3943
10. Adasme MF, Linnemann KL, Bolz SN, Kaiser F, Salentin S, Haupt VJ, et al. PLIP 2021: expanding the scope of the protein–ligand interaction profiler to DNA and RNA. Nucleic Acids Res. 2021 Jul 2;49(W1):W530–4. doi:10.1093/nar/gkab294

Figures

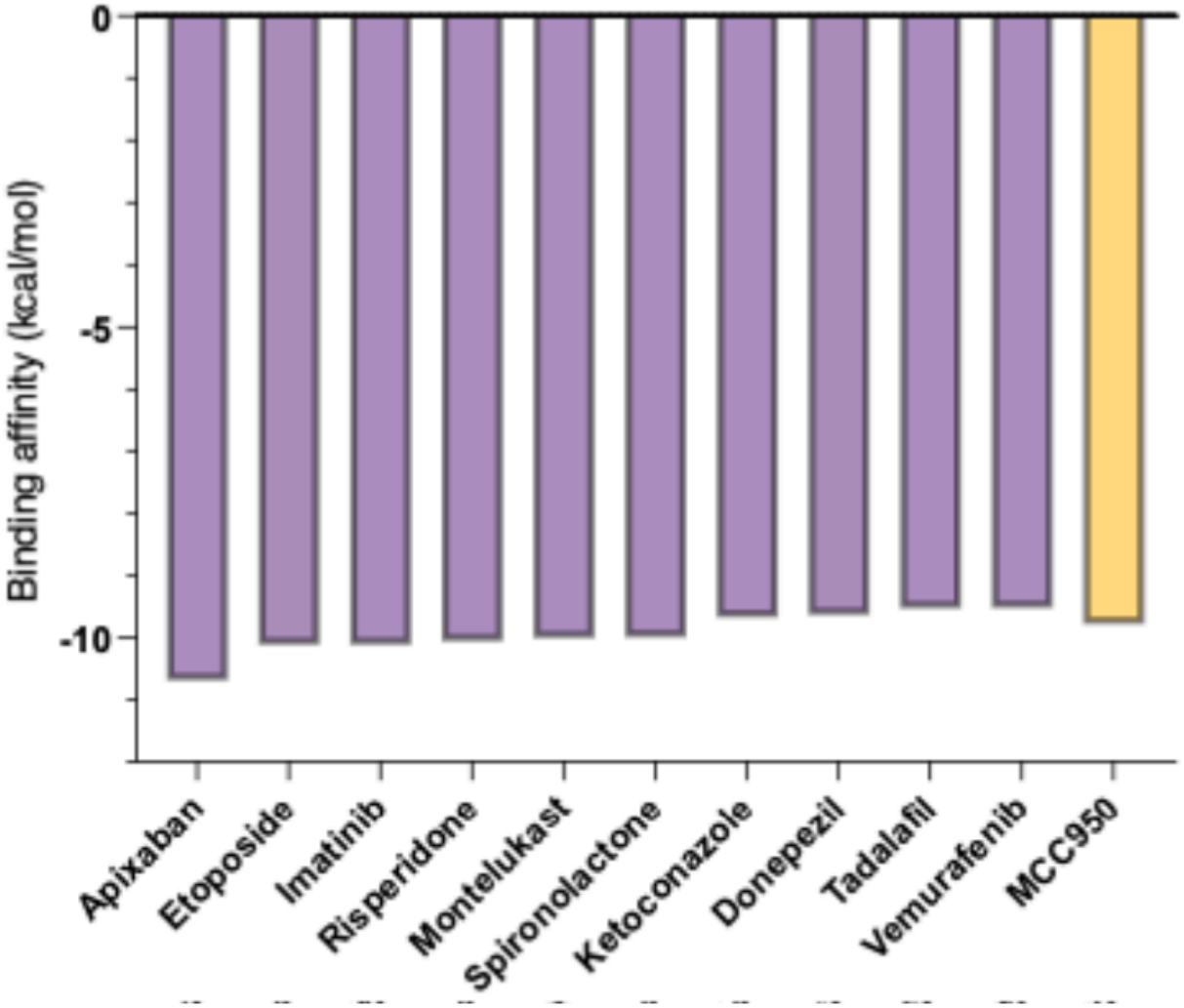


Figure 1

Comparative docking scores of the top ten FDA-approved compounds screened against the NLRP3 NACHT ATP-binding pocket. Bars represent predicted binding energies (kcal/mol) obtained using AutoDock Vina. MCC950 (gold) is shown as the benchmark inhibitor, while screened compounds are shown in purple. More negative values indicate stronger predicted binding.

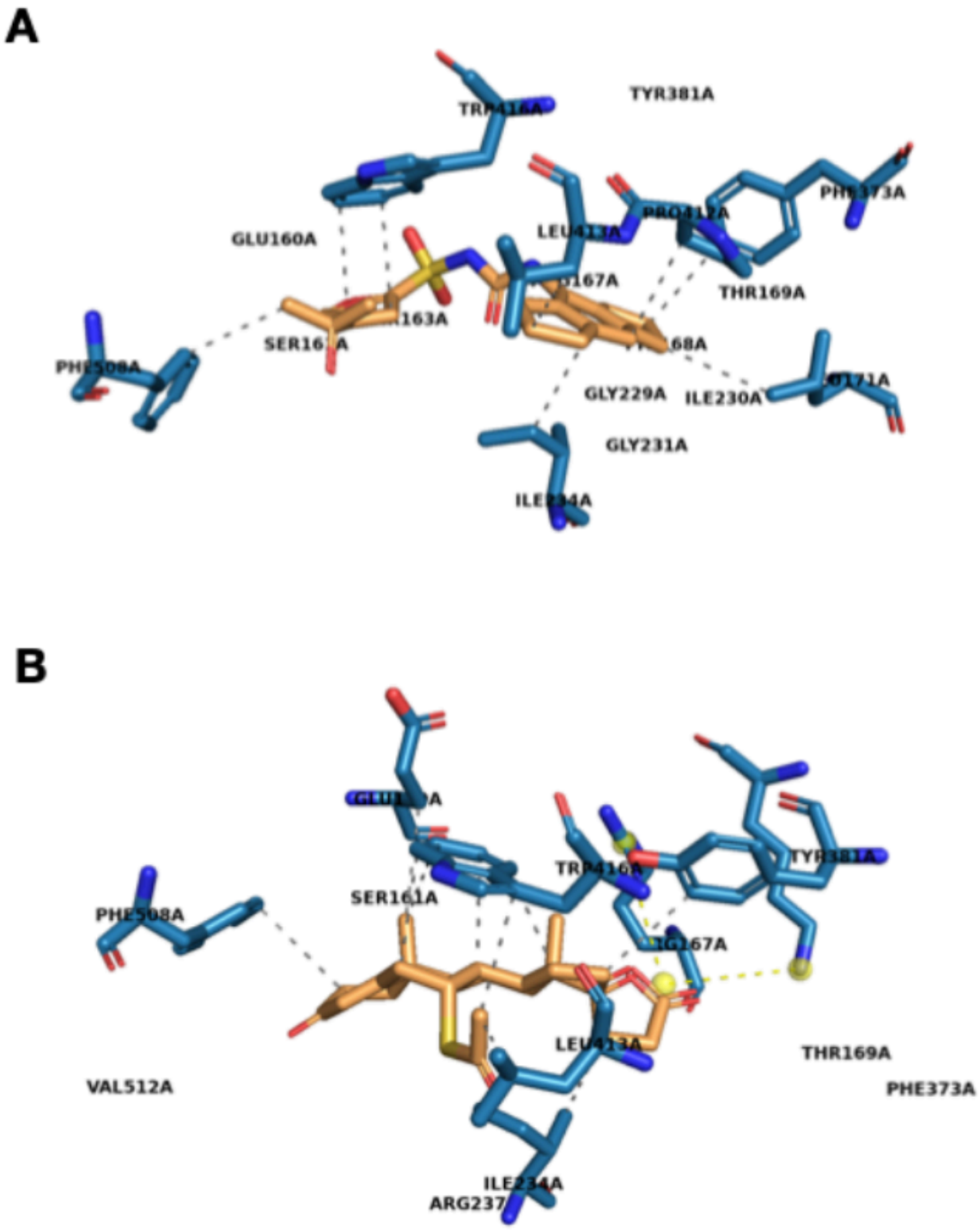


Figure 2

Predicted binding modes of MCC950 and Spironolactone in the NLRP3 NACHT ATP-binding pocket.

(A) MCC950 bound within the ATP-binding cavity adjacent to the Walker B motif. Hydrophobic interactions (grey dashed lines) involve ILE234, LEU413, TRP416, TYR381, PHE373, and PHE508. A hydrogen bond with Asp274 is observed.

(B) Spironolactone occupying a spatially overlapping pocket. Conserved hydrophobic contacts are maintained with the same core residues. A hydrogen bond with Asp274 and a salt bridge with ARG167 are observed (yellow dashed line).

Interactions were generated using PLIP and represent computational predictions.